Cathodic Delaminations of Poly(phenyl ether ether ketone) (PEEK) Coatings Overlaid on Zinc Phosphate-Deposited Steels*

T. SUGAMA† and N. R. CARCIELLO

Energy Deficiency and Conservation Division, Department of Applied Science, Brookhaven National Laboratory, Upton, New York 11973

SYNOPSIS

The melt-crystallized poly(phenyl ether ether ketone) (PEEK) polymer was overlaid on crystalline zinc phosphate (Zn · Ph) conversion coating-deposited and nondeposited cold-rolled steels at 400°C in air or in N_2 environments. The ability of these coating systems to protect the steel against corrosion was evaluated from the rate of cathodic delamination of the coating layer from the steel. Because the cathodic reaction, $H_2O + 1/2O_2 + 2e^- = 2OH^-$, at the corrosion side of a defect in the coating layer creates a high pH environment at the interfacial boundary between the coating and steel, the magnitude of susceptibility of the interfacial intermediate layers to the alkali-induced degradation played a key role in suppressing cathodic failure. The lowest level was observed in the N_2-induced PEEK/Zn · Ph/steel joint systems, thereby decreasing the rate of delamination. By contrast, oxidized PEEK induced by air in same joint systems was susceptible to the alkali-catalyzed hydrolysis. This phenomenon significantly promoted the alkali dissolution of Zn · Ph crystals, reflecting a high rate of delamination. Nevertheless, the introduction of Zn · Ph as interfacial tailoring material into the intermediate layers markedly acted in reducing the cathodic delamination of PEEK/steel joint systems. © 1993 John Wiley & Sons, Inc.

INTRODUCTION

We have investigated the characteristics of melt-crystallized poly(phenyl ether ether ketone) (PEEK) as an adhesive for steel-to-steel joints.[1] Knowledge of the interfacial chemistry that governs whether the adhesion will be poor or good at PEEK/cold-rolled steel (CRS) joints prepared under air or N_2 at 400°C led us to the following general conclusions: Although the oxygen-catalyzed deformation of PEEK in air gave a low degree of crystallinity, the PEEK favorably bound with the Fe_2O_3 at the top surface of CRS. However, the extensive formation of a mechanically weak Fe_2O_3 layer by a high degree of oxidation at the interfaces created an undesirable boundary region, indicating that failure occurs cohesively through this weak Fe_2O_3 layer. In N_2, two factors, (1) the formation of well-crystallized PEEK and (2) a moderate rate of $Fe \rightarrow Fe_2O_3$ conversion at interfaces, contributed significantly to strengthening the PEEK-to-CRS bonds. Despite improving bond strength, we proposed that the bonding failure of N_2-induced PEEK/CRS joint was an adhesive mode, in which delamination of the PEEK film occurs at the PEEK–CRS interfaces.

Based on this information, the experimental work was extended to evaluating PEEK as a coating material to protect steels from corrosion. We considered that the cathodic reaction, $H_2O + 1/2H_2O + 2e^- = 2OH^-$, occurs at the corrosion sites of steel in a near-neutral aqueous environment, underneath the coating layers. Thus, the emphasis of this paper was directed toward obtaining a better understanding of the chemical changes at the PEEK-to-CRS inter-

* This work was performed under the auspices of the U.S. Department of Energy, Washington, DC, under Contract No. DE-AC02-76CH00016, and supported by the U.S. Army Research Office Program MIPR-ARO-119-91 and the Physical Sciences Department of the Gas Research Institute, under Contract No. 5090-260-1948.

† To whom correspondence should be addressed.

Journal of Applied Polymer Science, Vol. 50, 1701–1713 (1993)
 CCC 0021-8995/93/101701-13

facial contact zones, which would be important in reducing the rate of alkali-catalyzed cathodic delamination of the PEEK film.

Although the zinc phosphate (Zn · Ph) conversion coatings are susceptible to alkali dissolution,[2] we also investigated the effectiveness of Zn · Ph, as an interfacial tailoring material between PEEK and CRS, in decreasing the rate of the cathodic delamination of PEEK film from the phosphatized CRS. The investigations involved the interfacial failure modes and bond strengths of the PEEK-to-phosphatized CRS joints prepared at 400°C in air and in N_2. This information was correlated directly to the results of the exploration of cathodic delamination.

EXPERIMENTAL

Materials

The metal substrate used was AISI 1010 CRS containing 0.08–0.13 wt % C, 0.3–0.6 wt % Mn, 0.04 wt % P, and 0.05 wt % S. The formulation of the Ni-modified zinc phosphate liquid was 1.3 wt % zinc orthophosphate dihydrate [$Zn_3(PO_4)_2 \cdot 2H_2O$], 2.6 wt % H_3PO_4, 1.0 wt % $Ni(NO_3)_2 \cdot 6H_2O$, and 95.1 wt % water.

In preparing the zinc phosphate (Zn · Ph) samples, the steel surfaces first were wiped with acetone-soaked tissues to remove any surface contamination from mill oil. The steel then was immersed for up to 20 min in the Zn · Ph conversion solutions at a temperature of 80°C. Finally, the deposited Zn · Ph layers were dried in an oven at 80°C for 2 h.

PEEK powder for the slurry coating was supplied by the Imperial Chemical Industry (ICI). The "as-received" PEEK was a finely divided, gray-colored powder having a high melt flow with a melting point of $\approx$ 350°C. The PEEK film was deposited on the surfaces of the CRS and Zn · Ph-treated steel substrate in the following way: First, the substrates were dipped into a PEEK slurry consisting of 45 wt % PEEK and 55 wt % isopropyl alcohol at 25°C. The slurry-coated substrates were heated in the air or in N_2 at 400°C for 2 h and then cooled to room temperature at the rate of −10°C/min.

Measurements

The chemical compositions and states present on a bond-failure site at the interfaces of PEEK/substrate joint systems before and after the cathodic tests were explored using scanning electron microscopy (SEM), energy-dispersion X-ray spectrometry (EDX), and X-ray photoelectron spectroscopy (XPS). XPS was done on a V.G. Scientific ESCA 3MK II. The excitation radiation was provided by an AlKα (1486.6 eV) X-ray source, operated at a constant power of 200 W. The vacuum in the analyzer chamber of the instrument was maintained at 10^{-9} Torr. The atomic concentrations and ratios for the respective chemical elements were determined by comparing the XPS peak areas, which were obtained from the differential cross sections for core-level excitation. To set a scale in all the high-resolution XPS spectra, the binding peak was fixed at 285.0 eV as the internal reference. A curve-deconvolution technique, in conjunction with a DuPont curve resolver, was employed to find the individual chemical states from the high-resolution spectra of each element.

The lap-shear tensile strength of metal-to-metal joints was determined in accordance with the modified ASTM Method D-1002. Before overlapping the metal strips (50 mm long and 15 mm wide), a 10 × 15 mm lap-area was coated with PEEK adhesive. The overlapped metal specimens were placed in an oven at 400°C for 2 h and then cooled to the room temperature at the rate of −10°C/min. The thickness of the overlapped PEEK film ranged from 25 to 75 μm. The bond strength of the lap-shear specimens is the maximum load at failure divided by the total bonding area of 150 mm^2.

The cathodic delamination tests for the PEEK-coated CRS and Zn · Ph specimens were conducted in an air-covered 1.0*M* NaCl solution, using an applied potential of −1.5 V vs. SCE for up to 8 days. We have given a schematic diagram of the test elsewhere.[3] A defect was made using a 1 mm-diameter drill bit. After exposure, the specimens were removed from the cell and allowed to dry. The PEEK coating was removed by cutting, revealing a delaminated region that appeared as a light gray area adjacent to the defect.

RESULTS AND DISCUSSION

Interfaces of PEEK-to-Zn · Ph Joints

Figure 1 shows the lap-shear bond strength at the Zn · Ph-to-Zn · Ph PEEK adhesive joints that were prepared by heating in air or in N_2 at 400°C for 2 h. For comparison, the bond strength at unphosphatized CRS-to-CRS PEEK adhesive joints was also determined. The data showed that the bond strengths depend primarily on the ambient atmo-

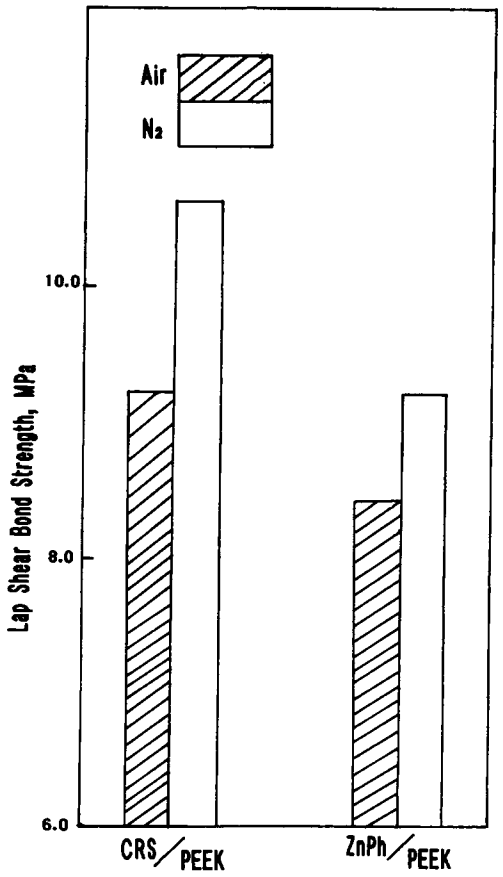

Figure 1 Lap-shear bond strength at Zn · Ph-to-Zn · Ph and CRS-to-CRS PEEK adhesive joints prepared in air or in N_2 at 400°C.

sphere during the melting–crystallization process of PEEK and on the species of substrate. In the CRS-to-PEEK joint systems, the strength of specimens prepared under N_2 is much greater than that of specimens made in air. As we discussed in our previous paper,[1] the reasons for the lesser strength of the air-treated specimens were due to two factors: (1) the extensive formation of mechanically weak Fe_2O_3 layers at the interface, and (2) the poor crystallization of PEEK film adjacent to the Fe_2O_3 caused by oxidation. A similar result was observed in the Zn · Ph-to-PEEK joint systems, namely, the bond performance of N_2-treated joints was better than that of those exposed to air. However, the bond strengths for both the N_2- and air-joint specimens with Zn · Ph were lower than those of the CRS-to-PEEK joints.

To ascertain the causes of good and poor interfacial bond performance for the Zn · Ph/PEEK systems after exposure to N_2 and to air, we removed the interfacial side of PEEK film from the phosphatized CRS in the joint systems made in air or in N_2 and explored it using the SEM, EDX, and XRD. Assuming that the bond failure may occur through the Zn · Ph layers or in the critical interfacial zones between PEEK and Zn · Ph, we investigated two reference XRD samples: Zn · Ph coating after heating at 400°C for 2 h in air and a PEEK film prepared at 400°C for 2 h in N_2. As represented in Figure 2, the *d*-spacing pattern (top) of 400°C-oxidized Zn · Ph reference sample revealed the presence of two different anhydrous Zn · Ph compounds—α-$Zn_3(PO_4)_2$ as a major phase and γ-$Zn_3(PO_4)_2$ as a minor one—both deriving from thermal dehydration of the original Zn · Ph hydrate phases, such as zinc orthophosphate dihydrate [$Zn_3(PO_4)_2 \cdot 2H_2O$] and hopeite [$Zn_3(PO_4)_2 \cdot 4H_2O$].[4] The formation of well-crystallized PEEK is recognizable from the typical features of the spacing pattern (bottom) of N_2-exposed film.[5] Figure 3 gives the results from SEM, EDX, and XRD analyses for the failure surface on the PEEK side obtained from N_2-induced joints. The SEM micrograph discloses rough surfaces containing a void. The XRD tracing (top) for this surface was recorded in the diffraction range 0.884–0.225 nm. According to XRD reference patterns (Fig. 2), the dominant spacing lines are assignable to the composition of three crystalline phases: PEEK, α-$Zn_3(PO_4)_2$, and γ-$Zn_3(PO_4)_2$.

The identification of such anhydrous α- and γ-phases adhering to the PEEK crystal coatings clearly verified that the dehydration causes the conversion of Zn · Ph hydrates into anhydrous Zn · Ph phases underneath the coating film during the melting–crystallization of PEEK. Also, there is a possibility that the melted PEEK fluid penetrated into the Zn · Ph layers because of the presence of PEEK crystal coexisting with the anhydrous Zn · Ph phases. However, no determination was made of the penetration depths of PEEK.

Of more interest, the hydrate → anhydrous phase transition of interfacial Zn · Ph layers in N_2 leads to the formation of the γ-$Zn_3(PO_4)_2$ phase, which is almost equal in amount to that of the α-phase (based upon the comparison between signal intensities). The EDX spectrum (bottom) accompanying the SEM showed the presence of Zn and Fe as the major elements present. By comparison with the XRD data, Zn could be associated with the α- and γ-$Zn_3(PO_4)_2$. Because the only source of Fe is the underlying CRS, the Fe detected on the failed surface may belong to Fe-based contaminants, in which the free Fe dissociated from CRS during precipitation of Zn · Ph on CRS surfaces was incorporated in the Zn · Ph layers.

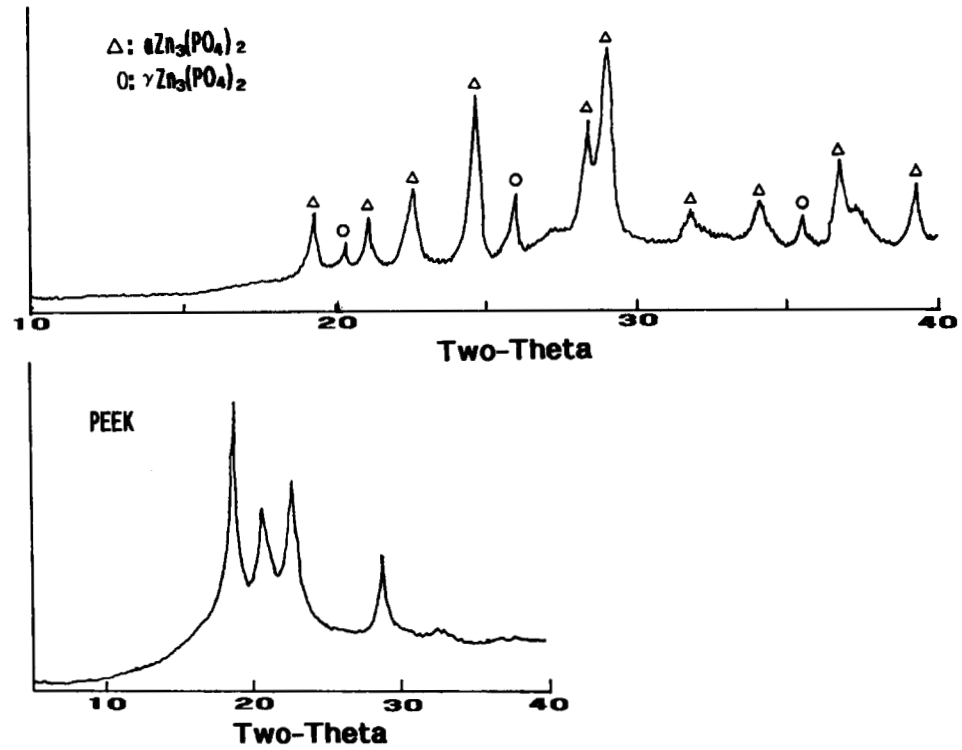

Figure 2 XRD patterns of the 400°C-oxidized Zn · Ph coating (top) and the PEEK film prepared at 400°C in N_2 (bottom) as reference samples.

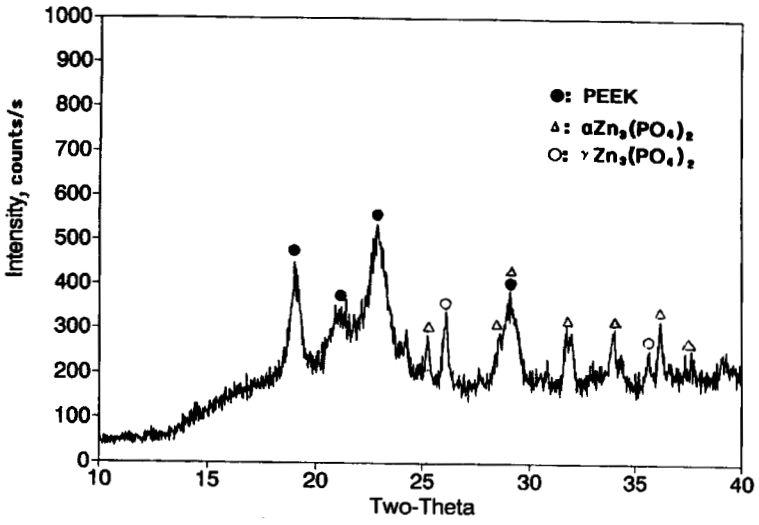

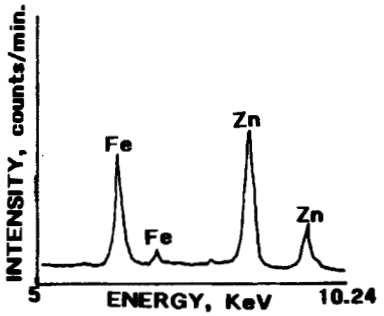

Figure 3 SEM, XRD, and EDX analyses of the PEEK side removed from phosphatized CRS in the PEEK/Zn · Ph/CRS joint system prepared in N_2.

From these data, it is reasonable to assume that the bond failure of N_2-induced PEEK/Zn · Ph joints occurs as a cohesive mode through the PEEK-penetrated Zn · Ph layers. This finding also suggests that the mechanical strength of Zn · Ph layers is lower than that of the adhesive force at the Zn · Ph-to-CRS joints. In the case of air-induced joints, there was a striking difference between the findings for air-induced joints (Fig. 4) and those from the N_2-induced joints, namely, (1) the SEM micrograph revealed a microstructure of continuous rough surface layers without any voids, (2) the EDX spectrum had an intense Fe signal and a low peak excitation of Zn, (3) the XRD lines for PEEK were weak, and (4) no γ-$Zn_3(PO_4)_2$ phase was found on the XRD pattern. The result, denoted by the second difference, suggests that the failed PEEK side contains a large amount of Fe. Since the XRD pattern of this sample does not show any crystalline phases of Fe-related compounds, the Fe atoms detected appear to be associated with amorphous Fe compounds that migrate from the CRS surfaces. The expression of a weak XRD line intensity (related to the third difference) represents the formation of poorly crystallized PEEK, reflecting the fact that the oxidation-catalyzed decomposition of PEEK in air at 400°C leads to a low degree of crystallinity.

To support these findings, we inspected, by XPS, the elemental compositions for cross-section samples of the PEEK/Zn · Ph joint systems prepared in N_2 and in air. The findings are given in Table I. In N_2, the PEEK side opposite the Zn · Ph had some Zn · Ph-related chemical components, such as P, Fe, and Zn atoms and a large amount of C belonging to the PEEK, suggesting that the failure occurs cohesively through the PEEK-penetrated Zn · Ph layers. By comparison, the failure side in the air-induced PEEK was characterized by the migration of more P, Fe, and Zn elements into the PEEK. Such a transference of a large amount of these elements results in the interfacial Zn · Ph side having a low concentration of residual P and Zn atoms and a high concentration of Fe.

To better understand the locus of failure, we attempted to identify the oxidation-induced Fe compounds that play a key role in promoting the failure

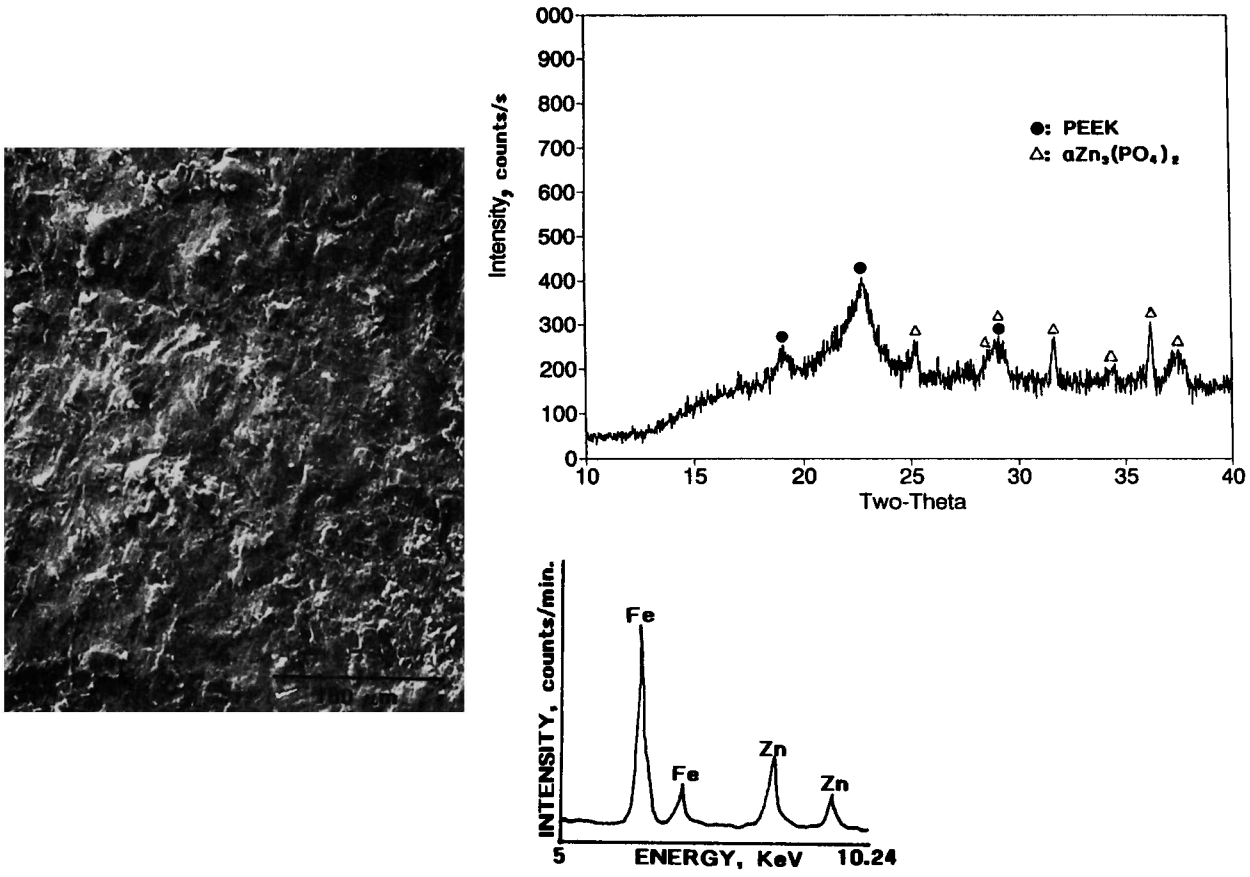

Figure 4 SEM, XRD, and EDX data of interfacial PEEK side in the 400°C-oxidized PEEK/Zn · Ph/CRS joint system.

Table I Atomic Concentration of N_2- and Air-treated PEEK/Zn · Ph/CRS Interfaces

Heating Environment	Failed Side	Atomic Concentration (%)				
		P	C	O	Fe	Zn
N_2	PEEK	11.2	47.5	37.3	2.5	1.5
N_2	Zn · Ph	8.0	56.0	29.2	3.7	3.1
Air	PEEK	15.4	28.2	46.3	6.6	3.5
Air	Zn · Ph	3.6	38.2	45.9	11.4	0.9

at the Zn · Ph-to-CRS joints. Our approach was to inspect the XPS $Fe_{2p3/2}$ core-level spectrum of the phosphatized CRS side removed from the PEEK. The binding energy (BE) was calibrated with C_{1s} of the principal hydrocarbon-type carbon peak fixed at 285.0 eV as an internal reference. The resultant $Fe_{2p3/2}$ region (not shown) indicated that the major core line at 710.8 eV originated from Fe in Fe_2O_3.[6] Thus, these data strongly supported our hypothesis that the locus of bond failure for air-induced PEEK/Zn · Ph/CRS joints is in the extensively formed Fe_2O_3 layers adjacent to the PEEK-mixed Zn · Ph layers. From this, possible explanations of why the bond strength of air-induced joint specimens is lower than that of N_2 specimens are as follows: the preparation of the PEEK/Zn · Ph joint system in hot air not only causes oxidation-induced decomposition of PEEK, but also creates a weak boundary region at interfaces between the PEEK-penetrated Zn · Ph layer and the CRS substrate. Thus, the incorporation of a large amount of oxygen into the interfacial Zn · Ph–CRS zones leads to the formation of thick layers of highly oxidized Fe compounds at the interfaces. The mechanical strength of such Fe_2O_3 layers formed beneath the Zn · Ph layer is probably weaker than the bond strength at the interfaces between the Fe_2O_3 and the PEEK-penetrated Zn · Ph layers. Thus, bond failure occurs through this weak layer in the vicinity of the composite layers of PEEK-Zn · Ph.

Cathodic Delamination

For all the joints, the cathodically delaminated area at the CRS or Zn · Ph substrate sides can be clearly identified as a ringlike structure surrounding the defect (Fig. 5). The total areas of this ring were computed to estimate the rate of cathodic delamination of PEEK film from the substrates as a function of exposure times. Figure 6 gives the delaminated area of PEEK from the substrates after up to 8 days of cathodic testing. For PEEK/CRS joint systems in the absence of Zn · Ph, the rate of delamination of PEEK in either specimens made in air or N_2 progressively increases in the first cathodic tests for 24 h; beyond this time, the delamination gradually occurs with a prolonged cathodic time. The curve also indicates that the area of delamination for the air-induced joint system is larger than that for the systems made in N_2. The rate of delamination of this PEEK/CRS system was markedly reduced when Zn · Ph was deposited onto the CRS surfaces as the interfacial tailoring material. The delaminated values of $\approx 6 \times 10$ mm^2 and $\approx 1.4 \times 10$ mm^2 for the air– and N_2–PEEK/Zn · Ph systems, respectively, obtained after 8 days were $\approx$ 10 times lower than those for the PEEK/CRS systems prepared in air or N_2 after the same exposure. Although the rate of delamination slowly increases with time, a result similar to that of the PEEK/CRS systems was obtained: the delaminated area of N_2-induced joints was much less than that of air-induced ones. Why such a high rate of delamination occurs at the critical interfacial zones of the PEEK/CRS systems and in the air-induced joint systems for CRS/PEEK and Zn · Ph/PEEK systems is of particular interest.

To obtain this information, we explored by XPS and SEM–EDX the cathodically failed PEEK, Zn · Ph, and CRS interfaces for 8 day-exposed PEEK/CRS and /Zn · Ph systems. Figure 7 shows, in the PEEK/CRS systems, the SEM images of the failed CRS side for N_2- or air-induced specimens. No specific feature was observed in the delaminated area of N_2-made specimens [Fig. 7(a)]; there was no evidence for the presence of PEEK adhering to the CRS. This finding seems to demonstrate that the cathodic failure takes place at the interfacial CRS side. Compared with this, the SEM micrograph of air-made specimens [Fig. 7(b)] was characterized by a topographical feature that shows a discontinuous coverage of PEEK film over the CRS, suggesting that cohesive failure in the PEEK layers can be the result of a cathodic-induced delamination mode. Table II gives the elemental compositions for both interfacial failure sides in the N_2- or air-made PEEK/CRS joint systems after cathodic tests for 8 days. For the N_2 systems, the cathodically removed PEEK side consists of 6.6% Cl, 55.9% C, 29.1% O, 6.7% Fe, and 1.7% Na. The incorporation of Cl and Na can be directly related to the penetration of NaCl electrolyte into the failure zones. The C belongs both to carbons in the PEEK and in the contaminants, whereas O may reflect the oxygen in PEEK and in Fe–oxide compounds. The detection of a certain amount of Fe on the PEEK interface demonstrated that this element migrates from the CRS to the

Figure 5 SEM micrograph of cathodically delaminated substrate side.

coating sides during the cathodic failure of the bond. The CRS interface had a lower concentration of C and Cl, a higher content of O and Na, and a similar amount of Fe compared to that on the PEEK side. Thus, the locus of failure appears to be the cohesive mode (in the CRS).

The air-made joint systems showed striking differences from the N_2 systems: (1) No Fe atom was found on the failed PEEK sides, (2) a large amount of C migrated from the interfacial PEEK sides to the CRS sides, (3) relatively little Fe was detected on the CRS sides, and (4) a lower penetration of Cl atom was observed, while there was still about 9% Na on both the delaminated PEEK and CRS sides. These results clearly revealed that the failure must occur through the PEEK layers adjacent to CRS.

To verify this finding, we next inspected the high-resolution C_{1s} and $Fe_{2p3/2}$ core-level spectra of the CRS interfacial sides delaminated from PEEK for both joint systems. The C_{1s} region of N_2- and air-prepared bulk PEEK film surfaces were the XPS reference samples; the results are illustrated in Figure 8. Spectral deconvolution in the C_{1s} region for the N_2-made PEEK reference film denoted as (a) showed four resolvable peaks at the position of binding energy (BE) of 285.0, 286.5, 287.6, and 291.5 eV. According to the literature,[7-9] the principal component at 285.0 eV reflects carbon in an aryl group. The assignments of the peaks at 286.5 and 287.6 eV as minor components are due to C in ether (C—O—C) and in ketone (C=O), respectively; the component at 291.5 eV is attributable to the $\pi \rightarrow \pi^*$ shake-up satellite peak of conjugated C=C bonds in the phenyl rings. For the air-made PEEK reference sample (b), the spectrum was characterized by a significant attenuation of the $\pi \rightarrow \pi^*$ shake-up peak at 291.5 eV, while maintaining almost the same peak position of the aryl carbons, C—O and C=O, at 285.0, 286.5 and 287.6 eV. A possible reason for the attenuation $\pi \rightarrow \pi^*$ is the breakup

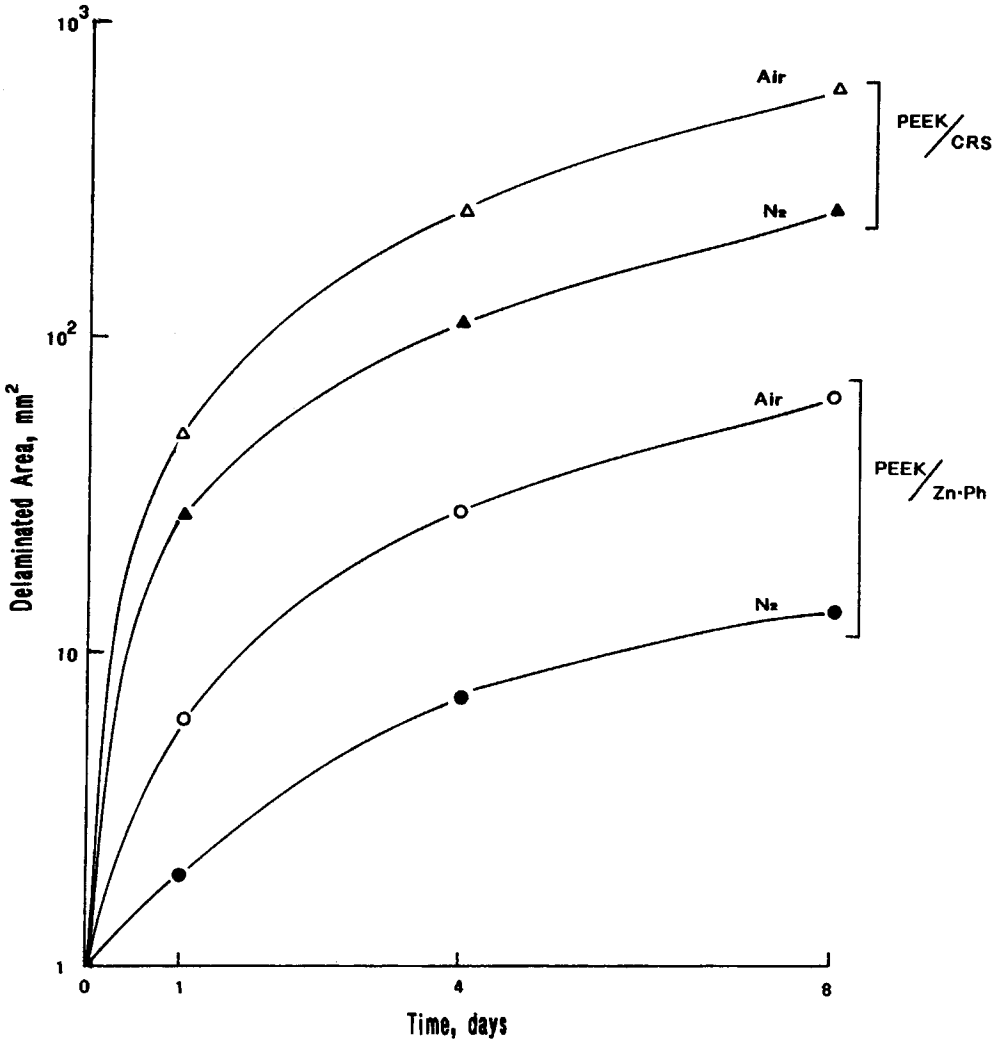

Figure 6 The cathodic delamination of PEEK film from CRS and Zn·Ph-deposited CRS substrates in the PEEK/CRS and PEEK/Zn·Ph/CRS joint systems prepared in air or in N_2 at 400°C.

of π bonds in the phenyl rings due to oxygen atoms impinging on the PEEK surfaces. By contrast, the spectral features (c) of the cathodically delaminated CRS side for the air-induced specimens expressed striking changes: (1) the overall decay of the C_{1s} signal, (2) the emergence of a new strong peak at 289.2 eV, and (3) the disappearance of the $\pi \rightarrow \pi^*$ component. The first and third results reflect the decay of ether, ketone, and aryl groups. The peak at 289.2 eV (the second change) is assignable to carbon originating from carboxyl groups ($-O-C=O$).[10]

Since the cathodic reaction, $H_2O + 1/2O_2 + 2e^- = 2OH^-$, occurring at the defect in the PEEK film, creates the alkaline environments underneath the coating, these data suggested that the deformation of PEEK structure caused by oxygen-catalyzed breakage of π bonds in the aryl groups and rupture of the ketone that directly links two phenyl rings not only inhibits the development of crystallinity, but also promotes the susceptibility of PEEK to the alkali-catalyzed hydrolysis. The latter phenomenon might lead to the formation of carboxyl groups from the hydrolysis-induced decomposition of PEEK.

Figure 9 shows the $Fe_{2p3/2}$ region for the cathodically failed CRS sides of the N_2- and air-induced joint specimens. The spectrum of the N_2-sample exhibited two resolvable peaks at 711.6 eV as the major component and at 710.8 eV as the minor one. The latter peak is assignable to the Fe originating from Fe_2O_3.[6] As reported by McIntye and Zetaruk,[11] the line excitation of the iron oxyhydroxide (FeOOH),

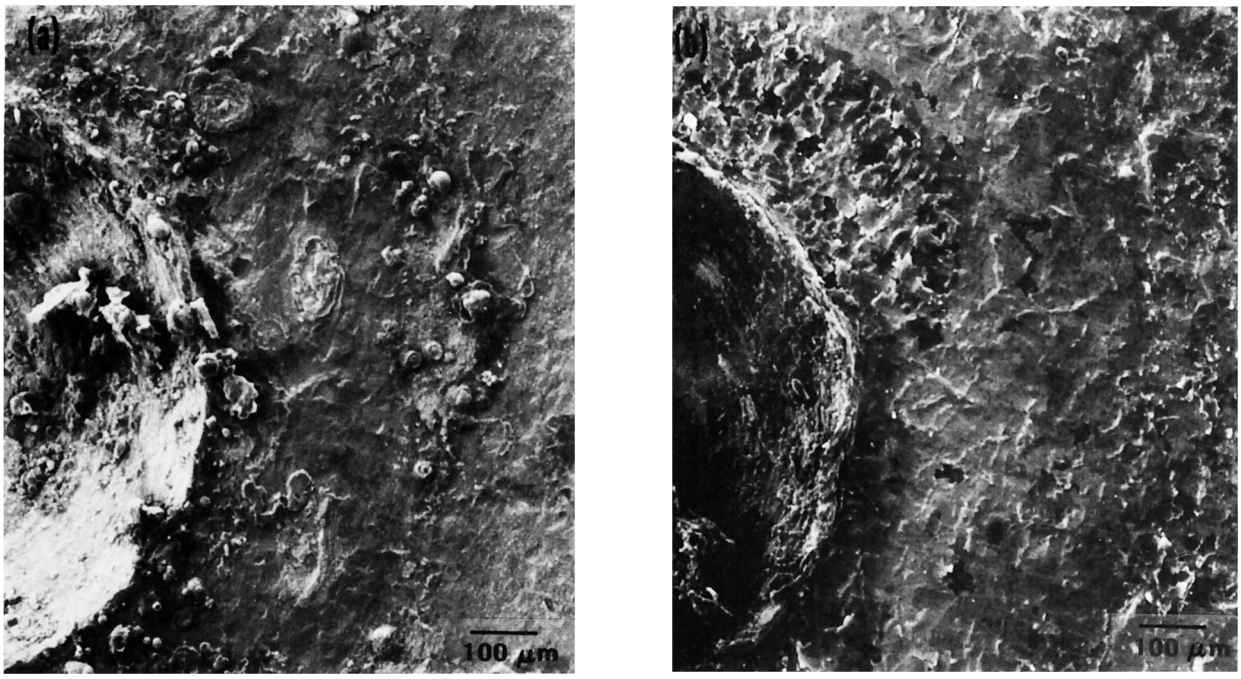

Figure 7 SEM micrographs of cathodically delaminated CRS interfaces for the (a) N_2- and (b) air-induced PEEK/CRS joint systems.

which is one of ferric rust compounds, occurs at a high BE site shifted by 0.85 ± 0.1 eV from that of Fe_2O_3. Thus, the main peak at 711.6 eV, corresponding to the shift of 0.8 eV above that of Fe_2O_3, may reveal the formation of FeOOH. In contrast, the spectral features of the air sample show that the main chemical state is Fe_2O_3, whereas the FeOOH is present as a minor component.

Taken together with the SEM observations, these XPS data clearly demonstrated that the mechanism of delamination caused by the cathodic reaction on the N_2-made joint system is quite different from that of the air-made system; the corrosion products formed (such as FeOOH) underlying the CRS substrate for the N_2-system promote the delamination of PEEK film from the CRS. By contrast, the cause of delamination in the air-system was due primarily to the alkali-catalyzed hydrolysis of oxidized PEEK film in the vicinity of the Fe_2O_3 layers. The latter failure mode resulted in a higher rate of delamination.

For PEEK/Zn · Ph/CRS joint systems, inspections both of the delaminated PEEK and Zn · Ph sides at interfaces were made with only the SEM–EDX analytical tool, because the delaminated area was too small to be investigated by XPS. Figure 10 shows the SEM–EDX findings from Zn · Ph and PEEK sides delaminated cathodically surrounding a defect in the air-induced joint system. The SEM image of Zn · Ph side (a) gave no evidence of crystalline Zn · Ph layers. In fact, the EDX spectrum of this area showed Fe as the major element and Zn as the minor one. No P element, belonging to Zn · Ph, was found in this spectrum. Of greater interest, the PEEK side that exhibits the rough surface microtexture (b) had a large amount of P and Na and a very little Fe, whereas no Zn element was detected.

As we reported previously,[2] a cathodic reaction occurring at a defect in the film in aqueous sodium chloride created a high pH environment of NaOH, formed by the charge valance between OH^- ions generated by the cathodic reaction and Na^+ ions from the electrolyte. The attack of such a strong alkali on the Zn · Ph layers underneath the polymeric top coatings caused the dissociation of a large amount of P from Zn · Ph layers, resulting in the alkali-induced dissolution of Zn · Ph crystals. From this information, the migration of P and Na atoms to the cathodically delaminated PEEK side can be interpreted as follows: The alkali-catalyzed hydrolysis of oxidized PEEK phase in the PEEK-penetrated Zn : Ph layers occurs near the defect, and, simultaneously, the P ions dissociated from the alkali dissolution of Zn · Ph in the hydrolyzed PEEK–Zn · Ph composite layers preferentially reacts with the Na ions of electrolyte to form a Na-related

Table II Chemical Composition of Interfacial Failure Sides after Cathodic Delamination Tests for PEEK/CRS Joint Systems Prepared in N_2 or in Air at 400°C

Heating Environment	Failed Side	Atomic Concentration (%) Cl	C	O	Fe	Na
N_2	PEEK	6.6	55.9	29.1	6.7	1.7
N_2	CRS	3.5	16.2	58.1	9.0	13.2
Air	PEEK	0.7	61.3	28.4	0.0	9.6
Air	CRS	1.5	32.3	55.0	2.5	8.7

phosphorous compound. Thus, substantial amounts of this Na—P reaction product remain in the PEEK layers.

We believe that the hydrolysis-related decomposition of the PEEK phase in the PEEK-Zn·Ph

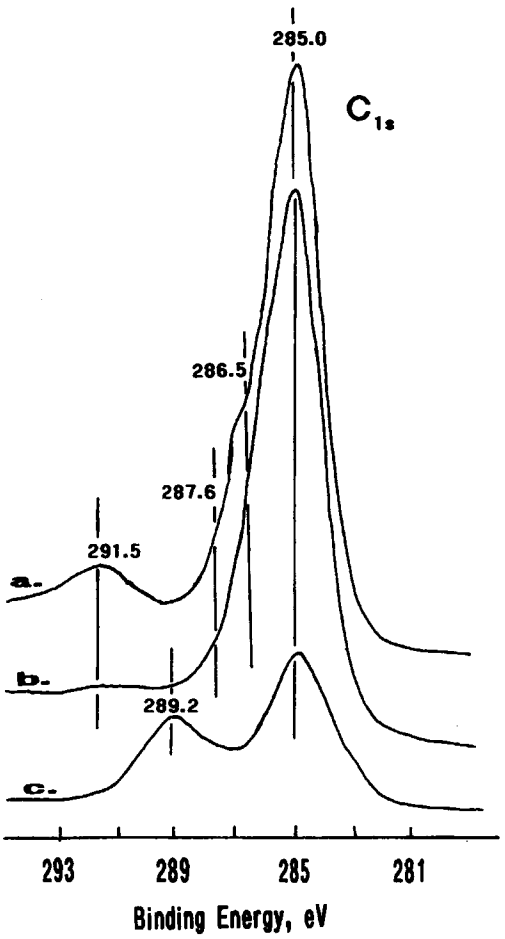

Figure 8 C_{1s} core level spectra for the (a) N_2- and (b) air-made bulk PEEK surfaces and (c) the delaminated CRS side after cathodic tests of PEEK/CRS joint specimens prepared in air at 400°C.

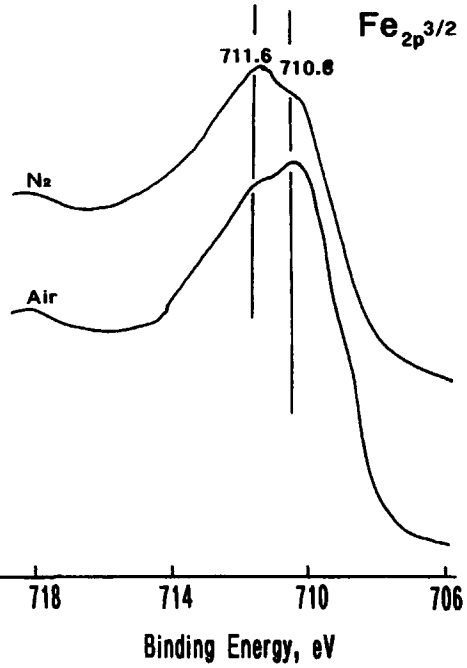

Figure 9 $Fe_{2p3/2}$ spectra of cathodically removed CRS sides for the N_2- and air-induced PEEK/CRS joint systems.

composite layers adjacent to the CRS increasingly promotes the alkali dissolution of Zn·Ph phase, reflecting the undesirable interfacial structure that is susceptible to disintegrations caused by the cathodic reaction. We paid considerable attention to the distinction between the morphological features of cathodically delaminated PEEK and Zn·Ph sides of N_2-treated joints (Fig. 11). The PEEK side (d) had an extremely rough surface, compared with that of the substrate side (c). As is evident from the microstructure of this rough surface, a massive number of Zn·Ph crystals seem to be transferred to the PEEK side from the CRS substrate during cathodic delamination. The EDX spectrum corresponding to the SEM clearly showed pronounced signals from P, Zn, and Ni originating from the Ni-modified Zn·Ph coatings, while an intense Fe signal, the principal element, also was present. The peak intensity of the Na element, which preferentially reacts with P liberated by alkali dissolution of Zn·Ph, was very weak, suggesting that even if the alkali dissolution of Zn·Ph occurs at defects the rate of dissolution is low. No Zn, P, and Ni signals were detected in the EDX spectrum of the substrate side (c); the major element was Fe, belonging to the CRS. The XPS $Fe_{2p3/2}$ region (not shown) of this sample revealed a peak at ≈711.6 eV, reflecting the formation of FeOOH. From this information, we

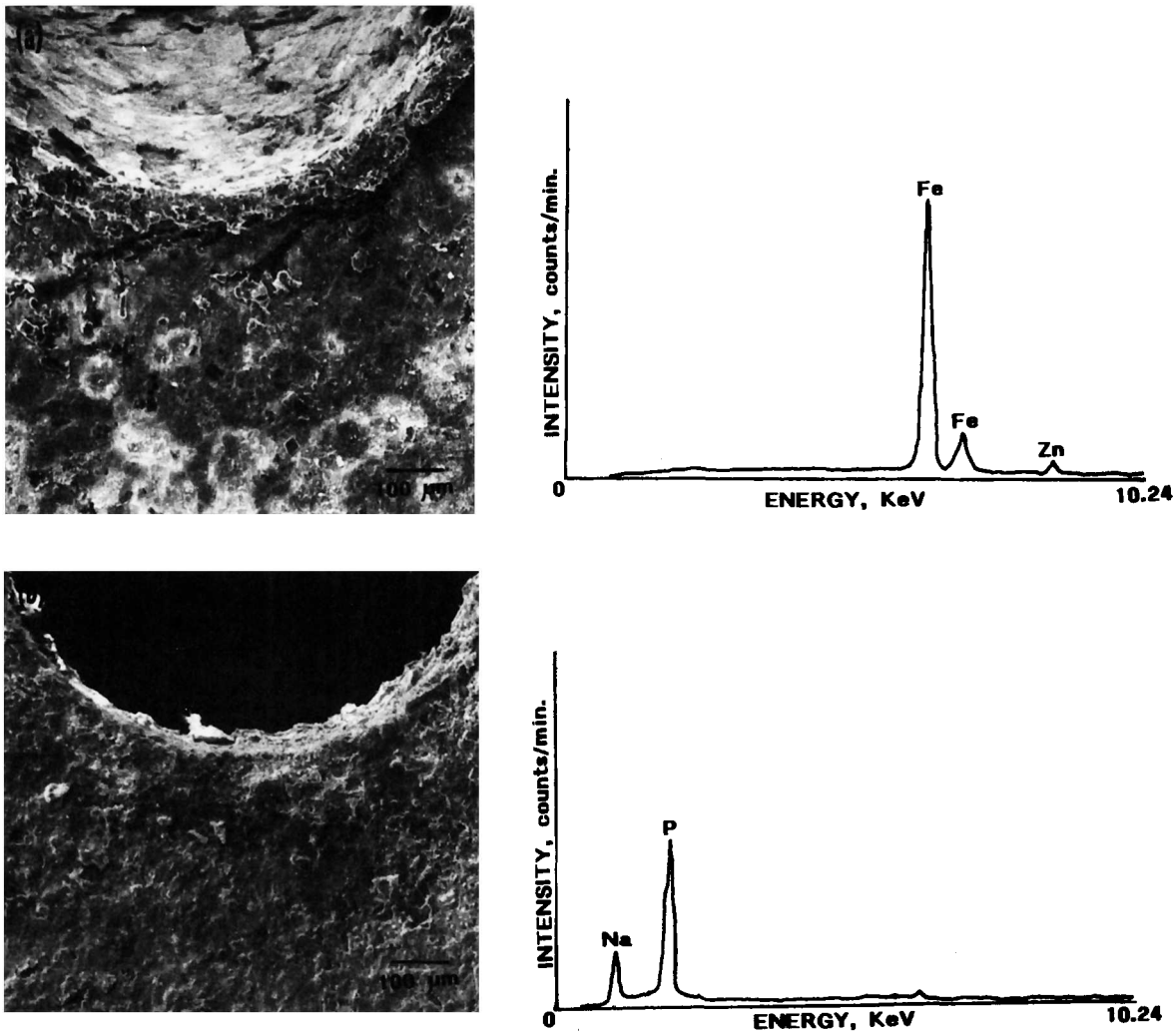

Figure 10 SEM–EDX inspections of (a) the cathodically failed substrate and (b) PEEK sides for the PEEK/Zn · Ph/CRS joint systems prepared in air at 400°C.

concluded that the cathodic delamination of N_2-made PEEK/Zn · Ph/CRS joint systems occurs through the buildup of FeOOH corrosion-product layers in CRS, underneath the PEEK–Zn · Ph composite layers. However, such a failure mode was responsible for reducing significantly the rate of cathodic delamination.

CONCLUSIONS

When the surface of crystalline zinc phosphate (Zn · Ph) conversion coating deposited on cold-rolled steel (CRS) was coated with a high-temperature-performance poly(phenyl ether ether ketone) (PEEK) polymer, we found that the locus and mode of bond failure depend mainly on the environment (400°C; N_2 or air) that was employed in the melt-crystallization and film-forming processes of PEEK slurry. In N_2, the bond failure was identified as a cohesive mode that occurs through the PEEK-penetrated Zn · Ph layers. Striking differences in the failure mode were observed from air-made PEEK/Zn · Ph/CRS joint systems, namely, the incorporation of hot air into the joint layers not only led to the oxidation-catalyzed decomposition of PEEK, reflecting a low rate of crystallinity, but also to the creation of weak boundary layers that were associated with the extensive Fe_2O_3 layers formed at the critical interfacial zones between the PEEK–Zn · Ph composition and the CRS substrate. Thus, the locus of failure was in the mechanically weak Fe_2O_3 layers close to the PEEK-mixed Zn · Ph layer; thereby, the

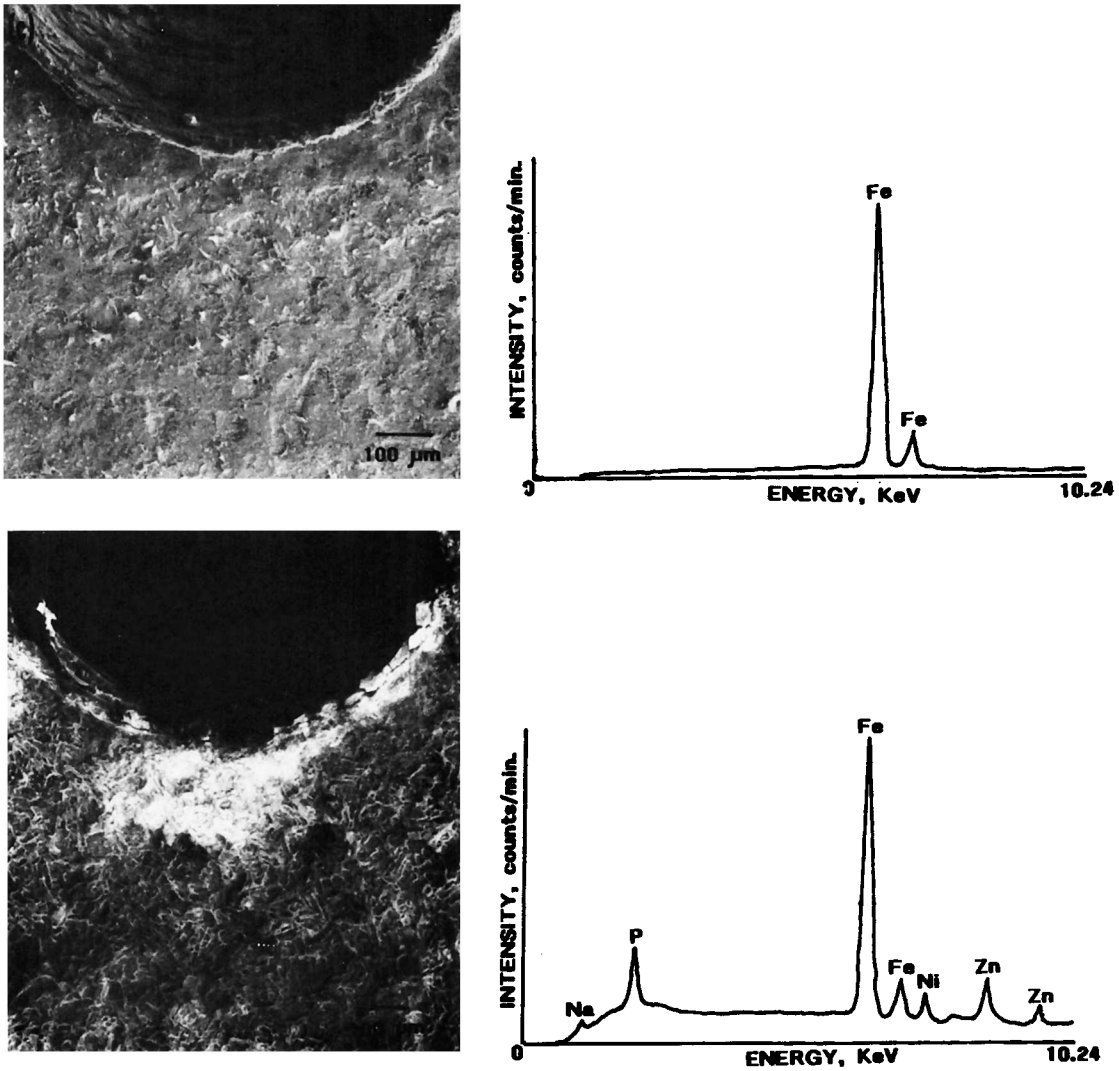

Figure 11 SEM–EDX data of (c) the cathodically failed substrate and (d) PEEK sides for the N_2-induced PEEK/Zn · Ph/CRS joint systems.

air-treated joint had a lower bond strength than did the N_2-induced joints. On the other hand, the crystalline Zn · Ph hydrate phase was converted into anhydrous α- and γ-$Zn_3(PO_4)_2$ phases during the melt-crystallization processes of PEEK at 400°C. Oxidation-induced phase conversion in hot air was particularly favorable for the formation of the α-phase.

Because of such a different interfacial bond failure and structure, attention was paid to the effect of PEEK-penetrated Zn · Ph coatings on the decrease in the rate of cathodic delamination, in which the attack of NaOH fluids caused by the charge valance between the OH^- ions from the cathodic reaction, $H_2O + 1/2O_2 + 2e^- = 2OH^-$ generated at the corrosion side near the defects, and Na^+ in the NaCl electrolyte causes separation of coating layers from the CRS substrates. The lowest rate of delamination was obtained from the N_2-induced joint system. The cathodic failure of this system occurred in the cathodically formed FeOOH corrosion product layers of the underlining CRS. In contrast, when the PEEK–Zn · Ph composite layers were prepared in air, the degradation caused by oxidation of PEEK promoted its alkali-catalyzed hydrolysis. This hydrolysis led to the dissociation of the P ion caused by the alkali dissolution of Zn · Ph crystals, thereby increasing the rate of cathodic delamination. Nevertheless, the rate of delamination of PEEK in the PEEK/CRS joint systems was significantly reduced by introducing Zn · Ph as the interface tailoring material into the intermediate layers between PEEK and CRS.

REFERENCES

1. T. Sugama, N. R. Carciello, and M. Miura, *Int. J. Adhes. Adhes.*, **12,** 27 (1992).
2. T. Sugama, L. E. Kukacka, N. R. Carciello, and J. B. Warren, *J. Coat. Tech.*, **61,** 43 (1989).
3. T. Sugama and N. R. Carciello, *J. Appl. Polym. Sci.*, to appear.
4. T. Sugama and J. Pak, *Adv. Mater. Manuf. Proc.*, **6,** 227 (1991).
5. P. C. Dawson and D. J. Blundell, *Polym. Rep.*, **21,** 577 (1980).
6. T. Sugama and N. R. Carciello, *Int. J. Adhes. Adhes.*, **11,** 97 (1991).
7. D. Briggs, D. M. Brewis, and M. B. Koniecyko, *J. Mater. Sci.*, **14,** 1344 (1979).
8. L. C. Lopey and D. W. Dwight, *J. Appl. Polym. Sci.*, **36,** 1401 (1988).
9. R. D. McElhaney, D. G. Castner, and B. D. Ratner, in *Metallization of Polymer*, E. Sacher, J.-J. Pireaux, and S. P. Kowalczyk, Eds., ACS Symposium Series 440, American Chemical Society, Washington, DC, 1990, pp. 370–378.
10. D. Briggs and M. P. Seah, *Practical Surface Analysis by Auger and X-ray Photoelectron Spectroscopy*, Wiley, New York, 1985, p. 385.
11. N. S. McIntyre and D. G. Zetaruk, *Anal. Chem.*, **49,** 1521 (1977).

Received June 1, 1992
Accepted April 12, 1993